Computational Optimization of Alkoxyamine-based Electrochemical Methylation

Fergus J.M. Rogers, Benjamin B. Noble,† and Michelle L. Coote*

ARC Centre of Excellence for Electromaterials Science, Research School of Chemistry, Australian National University, ACT 2601, Australia

ABSTRACT: Computational chemistry at the G3(MP2)-RAD//M06-2X/6-31+G(d,p)//SMD level of theory, was used to study the oxidation of a test set of methyl adducts of nitroxide radicals, as well as methyl adducts of Blatter's radical, a Kuhn verdazyl and two oxo-verdazyls. The barriers and reaction energies of the S_N2 reactions of the oxidized species with pyridine were also studied with a view to identifying species with both low oxidation potentials and low S_N2 barriers, so as to broaden the functional group tolerance of *in situ* electrochemical methylation compared with TEMPO-Me (1-methoxy-2,2,6,6-tetramethylpiperidine). Within the alkoxyamines, the oxidation potentials covered a range of 0.5 V, with trends explicable in terms of electrostatics, ring strain and charge transfer. The oxidation potentials of oxo-verdazyl adducts, verdazyl adducts and particularly the methyl adduct of Blatter's radical were considerably lower due to the ability of their extensive π-systems to stabilize a positive charge. As expected, the S_N2 reaction energies of the oxidized substrate became less favorable as the oxidation potential decreases. Unfortunately, this also meant that the barriers increased due to the excellent Evans-Polanyi correlation (R^2 = 0.92). Nonetheless, 7-methoxy-7-azadispiro[5.1.5^8.3^6]hexadecane, *N*,*N*-di-*tert*-butyl-*O*-methylhydroxylamine and particularly 1-methoxy-2,2,5,5-tetramethylpyrrolidine were identified as suitable candidates for broadening the scope of *in situ* electrochemical methylation while maintaining comparable kinetics to known reagents.

INTRODUCTION

Methylation is the addition of a methyl group to a substrate either directly or through replacement of a hydrogen atom. It is an important process in both organic synthesis and biology, where DNA methylation acts to change the activity of a DNA segment without altering the sequence.[1-6] In chemical synthesis, addition of a methyl group is typically achieved with nucleophiles, such as methyl lithium or Grignard reagents, or with radicals, while methyl substitution is achieved with strong electrophiles such as iodomethane, dimethyl sulfate, methyl triflate or diazomethane (or its derivatives). Unfortunately, there is trade-off between reactivity and risk as the best methylating agents tend to be acutely toxic, and many are also volatile and/or potentially explosive.[7] While safer and "greener" alternatives exist, they are less reactive.[8]

We recently introduced a new methylation procedure in which electrochemistry is used to generate a strong methylating agent *in situ*.[9] In our procedure, 1-methoxy-2,2,6,6-tetramethylpiperidine (TEMPO–Me), a stable and safe reagent, undergoes one electron oxidation. The oxidized species can then readily undergo an S_N2 reaction with nucleophiles, resulting in their methylation (Scheme 1A). The other product, a persistent nitroxide radical, is harmless and unreactive under these conditions. Calculations showed that the S_N2 reactivity of the oxidized TEMPO-Me with pyridine is better than that of methyl triflate and equivalent to that of the trimethyloxonium cation, two well-known powerful electrophiles. Experimentally, we showed that the procedure could deliver excellent isolated yields for methylation of a range of carboxylic acids, although for some substrates divided cells were necessary to prevent concurrent electroreduction of susceptible functional groups.

Despite this success, the high oxidation potential of TEMPO-Me (1.218 V vs Ag/Ag$^+$ in acetonitrile[10]; i.e., 0.79 V vs Fc/Fc$^+$ using the 0.425 V Fc/Fc$^+$ potential measured in the same experiment) places some limits on the substrate scope as many aromatic amines, phenols and organosulfur compounds will undergo competitive oxidation at this potential.[11] In the present work, we aim to examine whether other alkoxyamine derivatives, or indeed methyl adducts of other stable free radicals, such as triazinyl[12] and verdazyl [13, 14] radicals, will function in a similar capacity but at lower oxidation potentials.

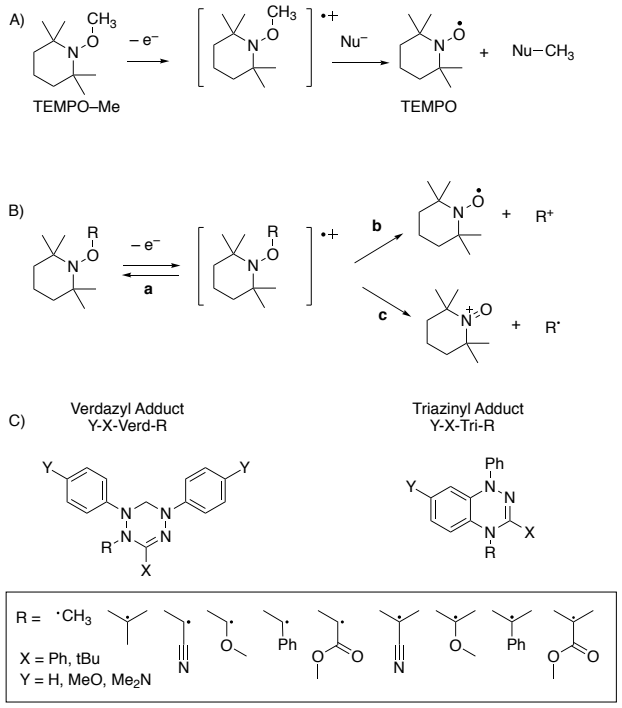

Scheme 1. (A) Methylation via oxidation of TEMPO-Me. [9] **(B)** Behavior of TEMPO-R in the absence of nucleophiles. Pathway a is favored for R= Me, Et, $CH_2OC(O)CH_3$; pathway b for R = 2-oxolane, Ac, $CH(CH_3)Ph$, i-Pr, t-Bu; pathway c for Bn, allyl, $CH(CH_3)C(O)OCH_3$, $C(CH_3)_2C(O)OCH_3$, $CH(CH_3)CN$.[10] Note that the reactivity of oxidized TEMPO-R is such that coordinating solvents and electrolytes will undergo S_N2 reactions analogous to the methylation procedure in (A).[15] **(C)** Verdazyl and triazinyl *R*-adducts examined previously. Their oxidation behavior is analogous to that of TEMPO-R, except that strongly electron donating substituents on the triazinyl or verdazyl moiety can convert them from a carbocation source to a carbon-centered radical source and vice versa for strongly electron withdrawing groups.[16, 17]

While the redox chemistry of nitroxides,[18, 19] triazinyls[20, 21] and verdazyls[22] has been well studied experimentally, the redox chemistry of their *R*-adducts has received only limited attention. Previously we have used theory and experiment to study the redox chemistry of TEMPO-R as a function of leaving group and reaction conditions, showing that when R is stable as a radical or carbocation it undergoes oxidative cleavage, but poor leaving groups like Me only undergo cleavage via S_N2 reactions with nucleophiles (Scheme 1B).[10, 15] It was this latter chemistry that led us to develop the aforementioned electrochemical methylation technique (Scheme 1A).[9] In following up these studies, we have used theory to evaluate triazinyl and verdazyl *R*-adducts for oxidative cleavage reactions (Scheme 1C). [16, 17] In the course of that work, we observed that the *R*-adducts of both triazinyls and verdazyls undergo oxidation at considerably lower oxidation potentials than the TEMPO-R adducts (−0.3 to 0.4 V vs Fc/Fc+ in acetonitrile for triazinyl adducts[16] and −0.7 to − 0.2 V for verdazyl adducts[17] versus 0.79 V vs for TEMPO-Me itself[10]). While this suggests the Me-adducts of triazinyl and verdazyl radicals could be good candidates for methylation at low oxidation potentials, it is important to remember that it is oxidation of the adduct that provides the energy required to activate it in the first place.[16, 17] Thus, it is instructive to investigate whether or not such savings in activation potential compromise S_N2 reactivity.

In the present work we examine whether structural variations to the nitroxide moiety can reduce the oxidation potential of the adduct, while maintaining sufficient S_N2 reactivity. The test set shown in Scheme 2 was chosen as it contains known nitroxides with a range of different ring sizes and substituents. Corresponding S_N2 barriers for the methyl adducts of Blatter's radical and the triphenyl Kuhn verdazyl species, in addition to two common oxo-verdazyls, (see Scheme 2) are also included. Herein oxidation potentials of these methyl adducts are calculated and compared with those of TEMPO-Me. At the same time, S_N2 reactivity of their methyl adducts with pyridine is calculated and compared with that of TEMPO-Me.

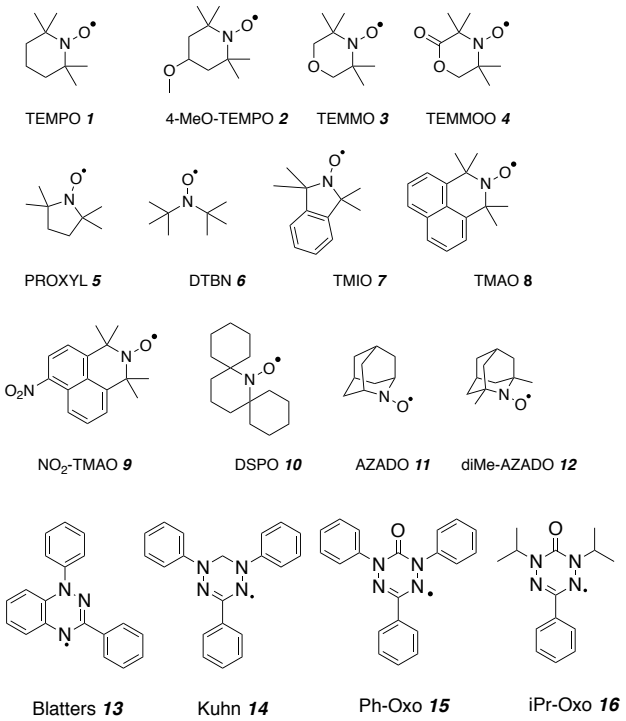

Scheme 2. Test set of nitroxide radicals and nitrogen-centred radicals considered to replace of TEMPO in TEMPO-Me.

COMPUTATIONAL METHODS

All standard ab initio molecular orbital theory and density functional theory (DFT) calculations were carried out using Gaussian 16 C.01[23] and Molpro 2019.2 [24] software packages. Procedures were chosen based on benchmarking against experiment in previous studies of similar systems, where they were shown to reproduce the experimental oxidation potentials of TEMPO-R alkoxyamines in acetonitrile to within a mean absolute deviation of 0.05V. [10, 25]

Geometries were optimized at the M06-2X/6-31+G(d,p)[26] level of theory, and frequencies were also calculated at this level. All geometries were verified as local minima (possessing no imaginary frequencies) save for transition states, which were identified with one imaginary frequency in the reaction coordinate. When appropriate, complete conformational searching was carried out based on the M06-2X/6-31+G(d,p) Gibbs free energies in solution. Improved single point energies were subsequently calculated using the high-level composite ab initio method G3(MP2)-RAD, in combination with the ONIOM partition scheme.[27] In these cases the respective core, shown in Figure S1 of the Supporting Information, was modelled with G3(MP2)-RAD while the remote substituents were modelled with M06-2X/6-31+G(d,p).

Gibbs free energies in solution were calculated via a thermocycle in which Gibbs free energies in the gas phase, as calculated via standard ideal gas partition functions, were combined with Gibbs free energies of solvation and the necessary phase change correction term.[28] The SMD solvent model[29] was used to correct for implicit solvent effects in acetonitrile. For this purpose, geometries were fully optimized in solution at the M06-2X/6-31+G(d,p) level.

Standard oxidation potentials (E_{ox}) in acetonitrile of the *methyl adducts* of all species in Scheme 2 were calculated via the Nernst equation against the Fc/Fc^+ couple in acetonitrile. The electron was treated under the EC-FD convention as described in Ref. [30] To maximize error cancellation, an isodesmic method was followed in which the experimental oxidation potential of TEMPO-Me in acetonitrile (0.79 V vs Fc/Fc^+) was used as the reference value.[10] To assist in the analysis of the results, reduction potentials of the *radicals* in Scheme 2 were also calculated. These are conditional formal potentials, rather than experimental half wave potentials, that do not account for protonation of the reduced product.

RESULTS AND DISCUSSION

The oxidation potential of the methyl adducts of the species in Scheme 2 are presented in Table 1, alongside the Gibbs free energy barriers and reaction energies for the S_N2 reaction of the resulting oxidized species with pyridine as a common nucleophile. Figure 1 shows a plot of the S_N2 barrier versus the oxidation potential. The fitted line represents regression analysis of the results of the nitroxide adducts only and with 3 of them also omitted as outliers (TEMMOO, AZADO and diMe-AZADO). These outliers, as well as the 4 non-nitroxides, are all labelled individually in Figure 1, and when these omitted the R^2 value is 0.93; even if just the 3 nitroxide outliers are included R^2 drops below 0.50. Figure 2 shows the barrier of the S_N2 reactions versus their reaction energies. These show a good Bell-Evans-Polanyi correlation over the entire dataset (R^2 = 0.92).

Table 1. Oxidation potentials (E_{ox}) of R-Me, and Gibbs free energy barriers and reaction energies ($\Delta G^‡$ and ΔG_{rxn}) of the S_N2 reaction between $[R–Me]^{+\bullet}$ and pyridine[a]

R in R–Me [a]		E_{ox} V vs Fc/Fc^+	$\Delta G^‡$ kJ mol^{-1}	ΔG_{rxn} kJ mol^{-1}
TEMPO	1	0.79	68.7	-129.5
4-MeO-TEMPO	2	0.86	64.1	-137.6
TEMMO	3	0.92	63.9	-139.3
TEMMOO	4	1.07	69.5	-157.3
PROXYL	5	0.56	76.6	-124.6
DTBN	6	0.70	68.4	-128.6
TMIO	7	0.74	69.5	-138.0
TMAO	8	1.00	56.0	-151.0
NO_2-TMAO	9	1.07	57.5	-158.2
DSPO	10	0.70	70.4	-130.7
AZADO	11	0.64	91.7	-99.7
diMe-AZADO	12	0.86	73.7	-122.0
Blatters	13	-0.08	143.5	-33.9
Kuhn	14	0.31	137.6	-48.6
Ph-Oxo	15	0.64	110.0	-94.0
iPr-Oxo	16	0.55	110.5	-106.1

[a]See Scheme 2 for chemical structures.

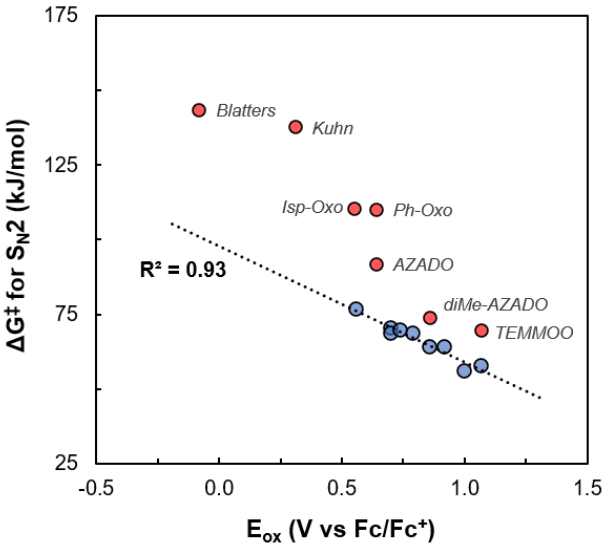

Figure 1. The $\Delta G^{\ddagger}$ for the S_N2 process (evaluated at 25°C, in kJ mol^{-1}) versus oxidation potential (in V versus Fc/Fc$^+$). The trend line is fitted to all points except the outliers marked (red circles). Even if only the nitroxide outliers are included the R^2 drops below 0.5.

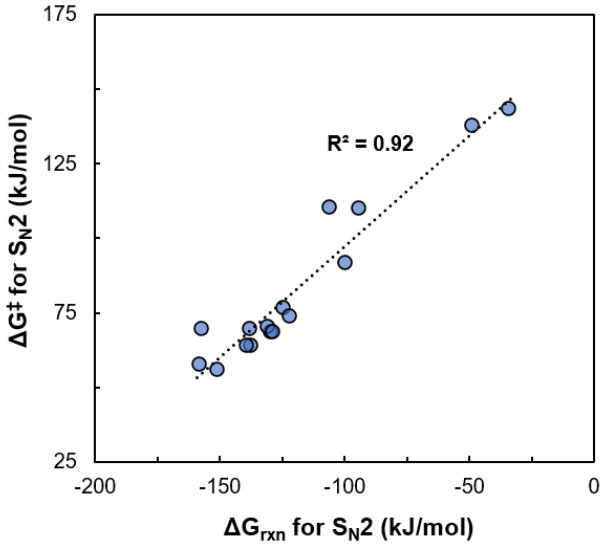

Figure 2. The $\Delta G^{\ddagger}$ for the S_N2 process versus the corresponding reaction energy, ΔG_{rxn} (both evaluated at 25°C, in kJ mol^{-1}). The trend line is fitted to the entire dataset.

From Figure 1, it is seen that, broadly speaking, the lower the oxidation potential, the higher the S_N2 barrier. This is unsurprising as there is a direct thermodynamic link between the lowering of the oxidation potential and the lowering of the S_N2 reaction energy (Figure 3) and, by an Evans-Polanyi rule extension, also the S_N2 barrier. From Figure 3, it is seen that the greater the oxidation potential of the substrate the greater the difference between the S_N2 barriers of the neutral and oxidized species. However, this difference also depends on the reduction potential of the leaving group – the harder it is to reduce the leaving nitroxide or hydrazyl radical, the lower the reaction energy in the oxidized form.

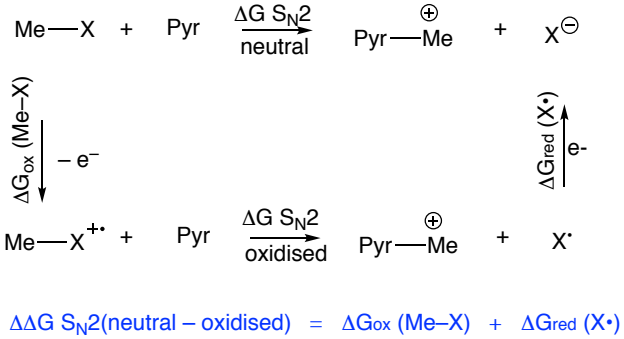

Figure 3. Thermodynamic cycle relating change in S_N2 reaction energy between neutral and oxidized form and the oxidation potential of the neutral substrate and reduction potential of leaving radical.

A simple way of thinking about this is that the neutral adduct is unreactive to S_N2 reactions and so energy has to be put into it to active it – the more energy you put in, the more reactive it becomes. By Hess's law, the energy you put in is the difference between the oxidation potential of the adduct and reduction potential of the corresponding nitroxide or hydrazyl radical (Figure 3). If the oxidation potential of adduct is low or the reduction potential of the radical is high, less energy is put in and the oxidized adduct is less reactive. The correlation between S_N2 reactivity and oxidation potential in Figure 1 suggests that for most species, oxidation potential of the adduct and reduction potential of the radical are well correlated. The outliers in Figure 1 are species where this correlation breaks down.

These outliers in Figure 1 all have barriers larger than would be expected based on the oxidation potential alone; thus, they should have higher reduction potentials than expected based on their oxidation potentials. Indeed, when the relative oxidation potential (versus TEMPO) is plotted as a function of the corresponding relative conditional formal reduction potential, the 5 *worst* outliers in Figure 1 are the same 5 outliers (see Figure 4, data in Table S1 of the Supporting Information). In all cases their reduction potentials are considerably higher than the trend line, indicating that the stability of the anion is significantly lower than otherwise expected based on how those functional groups affect the oxida-

tion potential of the adduct. Unsurprisingly, these outliers are primarily the nitrogen centered species, which are less able to bear a negative charge than the oxygen center of the nitroxides. In those cases, the reduction potentials over-estimate the stability of the radicals (and hence the driving force of the reaction) compared with the other species.

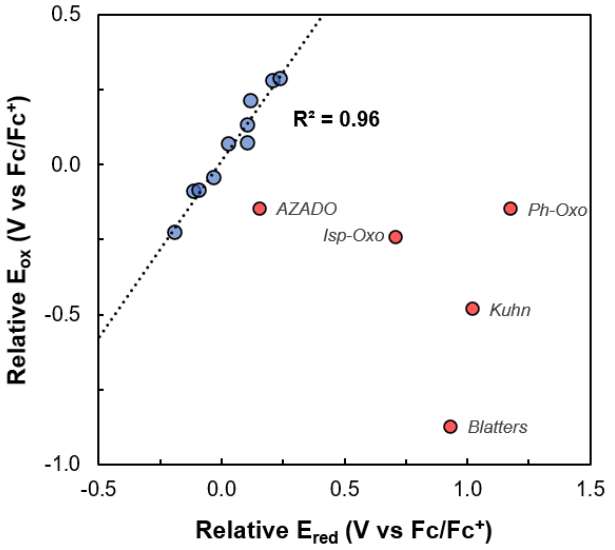

Figure 4. Relative oxidation potential of the Me-adducts (relative to TEMPO-Me, V) versus the corresponding relative reduction potential of the radicals (relative to TEMPO, V). The trend line is fitted to all points except the outliers marked. Note that conditional formal reduction potentials were calculated, and do not reflect the effects of subsequent protonation of the reduced form.

Structure-Reactivity Analysis. The S_N2 barriers of the oxidized species largely follow expectations based on their thermodynamics, which are in turn related to their oxidation and reduction behavior. Another way of thinking about these trends is in terms of how stable the substrate is as a cation (the less stable, the more reactive) and how stable the product radical is (which is reflected in how hard it is to reduce, at least among the nitroxides). These govern the thermodynamic driving force of the reaction, and given the Evans-Polanyi correlation, also the barriers.

As for the trends in the oxidation potentials of the methyl-adducts themselves, the large difference between alkoxyamines and the aromatic amines is the enhanced ability of the latter to stabilize a positive charge via resonance delocalization. The alkoxyamine subset is very structurally diverse and was deliberately chosen so to assess how different chemical features (e.g. cyclic vs acyclic, 5- vs 6-membered rings, saturated vs unsaturated rigidification) influenced oxidation behavior and reactivity. While this diversity precludes quantitative analysis based on a single variable (e.g. an electrostatic descriptor), semi-qualitative and qualitative analysis reveals there are several important structural features that can impact alkoxyamine oxidation.

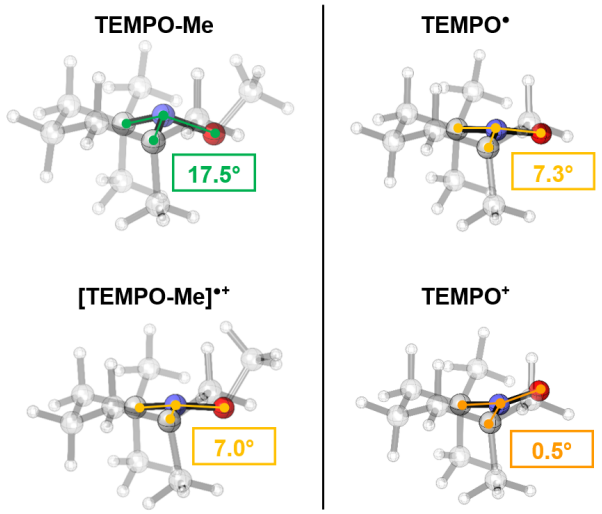

Figure 5. N-Pyramidalization angles of TEMPO-Me and TEMPO-Me$^{\bullet+}$, compared with TEMPO$^{\bullet}$ and TEMPO^{+}. Calculated using the POAV approach. [31]

Firstly, by comparing TEMPO-Me and PROXYL-Me, we note that ring size is clearly an important factor influencing alkoxyamine oxidation. Indeed, this ring contraction lowers E_{ox} by 230 mV. A similar decrease is also observed moving from TMAO-Me to TMIO-Me, with E_{ox} lowered by 260 mV. This suggests that alkoxyamine oxidation is reasonably sensitive to ring size, which is somewhat in contrast to nitroxide oxidation. Indeed, previous theoretical calculations indicate that the oxidation potentials of the corresponding TEMPO and PROXYL nitroxides are nearly identical, though their reduction potentials differ by around 140 mV.[32] This result can be rationalized on the basis that alkoxyamines undergo more significant geometry relaxation upon oxidation than nitroxides (see Figure 5).

As Figure 5 illustrates, the TEMPO-Me alkoxyamine adopts a nearly pyramidal geometry around the N atom, with a CNC bond angle of 118.5° and an N-pyramidalization angle of 17.5°. The corresponding radical-cation adopts a more planar geometry, with a CNC bond angle of 126.6° and an N-pyramidalization angle of 7.0°. In

contrast, both TEMPO and its corresponding oxoammonium cation have reasonably planar geometries, with CNC bond angles of 124.0° and 124.4°, respectively. Moreover, the N-pyramidalization angles for TEMPO and its respective oxoammonium cation are also more comparable (7.3° and 0.5°, respectively). As particular cyclic scaffolds possess inherent structural preferences, oxidation and reduction reactions that involve large geometry relaxations are obviously more sensitive to ring size. [18, 32, 33] The lower oxidation potential of PROXYL-Me vs TEMPO-Me suggests that a pyramidal type N-atom is more destabilized by pyrrolidine ring when compared to a piperidine. Consistent with this notion, the reduction potential of the PROXYL nitroxide is 140 mV lower than TEMPO,[32] indicating that the corresponding (pyramidal) oxyamine anion is less stable for PROXYL than TEMPO.

Having established the importance of ring size, we next considered the impact of remote electrostatic effects. We previously developed a simple descriptor for describing oxidation of nitroxide *radicals* in terms of the electrostatic effects of their remote substituents.[19] Though our equation was limited to cyclic nitroxides bearing identical (tetramethyl) alpha substitution, it was successful in rationalizing a large set of different nitroxide frameworks, including those based on pyrrolidines, pyrrolines, isoindolines, piperidines, morpholines, azaphenalenes and azepines. This previous nitroxide set encompassed 5-,6- and 7-membered cyclic nitroxides and incorporated rings with both saturated and unsaturated functionality. The descriptor was calculated by placing the same substituents in the corresponding carbocycle (through a CH_2/NO substitution) to estimate the dipole and quadrupole moment caused by the substituent alone.

Obviously, the sensitivity of alkoxyamine oxidation to ring size precludes similar quantitative electrostatic analysis over the entire alkoxyamine subset. Moreover, the inclusion of acyclic species and changes in hyperconjugation also somewhat confound this analysis. These considerations aside, electrostatic effects of the remote substituents do still play a significant role in influencing the alkoxyamine oxidation potentials. For instance, the trend TEMMOO-Me > TEMMO-Me > 4-MeO-TEMPO-Me > TEMPO-Me can be predominantly attributed to the progressively lower substituent dipole. This in turn lowers unfavorable charge-dipole interactions between the substituent and the forming NOR radical-cation. Similarly, both TMAO-Me and TMIO-Me possess notably higher oxidation potentials than their fully saturated analogues, TEMPO-Me and PROXYL-Me. In both cases, this higher oxidation potential can be attributed to the unfavorable electrostatic interaction between the substituent (aromatic) quadrupole and the forming NOR radical-cation. Similar electrostatic behavior was previous observed in nitroxide oxidation.[19]

From a practical point of view, the aim of the study was to identify suitable methylation agents with lower oxidation potentials than TEMPO so as to broaden the scope of our electrochemical methylation procedure. It is clear from Figure 3 that any lowering of the oxidation potential is accompanied by compromises to S_N2 reactivity. That said, both DSPO and DTBN can lower the oxidation potential requirements by 0.1 V without significantly affecting the barrier, while PROXYL lowers the requirements by ca 0.25V with less than a 10 kJ mol^{-1} compromise in activation energy and would also be worth considering when functional group tolerance is a problem. The barrier for the methylation of pyridine by the oxidized alkoxyamine of proxyl is 76.6 kJ mol^{-1}; for comparison, the barrier for MeOTf, also a powerful methylating agent, in the same reaction is 73.2 kJ mol^{-1}.[9]

CONCLUSION

Upon oxidation, alkoxyamines become powerful electrophiles, suitable for in situ methylation reactions. Previously we have developed this as an electrochemical synthetic technique using TEMPO-Me as the substrate.[9] Herein, using high-level quantum chemical calculations, we have studied the S_N2 activation barriers of a range of alkoxyamine derivatives, as well as methyl adducts of representative triazinyl, verdazyl and oxo-verdazyl adducts, to identify improved reagents capable of undergoing oxidation at lower potentials. Unfortunately, there is a strong correlation between the barrier and the oxidation potential; nonetheless, DSPO, DTBN and particularly PROXYL are capable of expanding functional group tolerance with minimal compromise to activity.

Moreover, those species with high S_N2 barriers are predicted to undergo reversible oxidation and are therefore promising in battery applications. Nitroxides[34-37] and verdazyls[38] have garnered significant attention in the context of organic batteries.[39 40] The former undergo reversible oxidation, the latter reversible oxidation and reduction. Recently, it has been suggested that Me-adduct of TEMPO could provide superior performance in this context due to its higher oxidation potential and thus greater energy storage capacity.[41] However, its S_N2 reactivity with solvent and electrolyte upon oxidation could potentially compromise battery lifetime.[15] Some of the

less reactive alkoxyamines studied here could thus provide a better compromise between stability and high oxidation potential.

ASSOSCIATED CONTENT

Supporting Information. Complete computational details. The supporting Information is available free of charge via the Internet at http://pubs.acs.org.

AUTHOR INFORMATION

Corresponding Author

* Email: michelle.coote@anu.edu.au

Current Address

†School of Engineering, RMIT University, Melbourne, Victoria 3001, Australia

Funding Sources

Australian Research Council (FL170100041)

ACKNOWLEDGMENT

MLC gratefully acknowledges a Georgina Sweet ARC Laureate Fellowship (FL170100041), generous allocations of supercomputing time on the National Facility of the Australian National Computational Infrastructure and preliminary studies by Ngoc Vu.

REFERENCES

1. Chen, Y., Recent Advances in Methylation: A Guide for Selecting Methylation Reagents. Chem. – Eur. J. 2019, 25, 3405-3439.
2. Luo, M., Chemical and Biochemical Perspectives of Protein Lysine Methylation. Chem. Rev. 2018, 118, 6656-6705.
3. Barreiro, E. J.; Kümmerle, A. E.; Fraga, C. A. M., The Methylation Effect in Medicinal Chemistry. Chem. Rev. 2011, 111, 5215-5246.
4. Schönherr, H.; Cernak, T., Profound Methyl Effects in Drug Discovery and a Call for New C-H Methylation Reactions. Angew. Chem. 2013, 52, 12256-12267.
5. Lamoureux, G.; Agüero, C., A Comparison of Several Modern Alkylating Agents. ARKIVOC 2009, 1, 251-264.
6. Carey, F. A.; Sundberg, R. J., Advanced Organic Chemistry 5th Ed. Springer: New York, 2007.
7. Sammakia, T., Diazomethane. In Encyclopedia of Reagents for Organic Synthesis, Wiley: 2001.
8. Tundo, P.; Selva, M., The Chemistry of Dimethyl Carbonate. Acc. Chem. Res. 2002, 35, 706-716.
9. Norcott, P. L.; Hammill, C. L.; Noble, B. B.; Robertson, J. C.; Olding, A.; Bissember, A. C.; Coote, M. L., TEMPO–Me: An Electrochemically Activated Methylating Agent. J. Am. Chem. Soc. 2019, 141, 15450−15455.
10. Hammill, C. L.; Noble, B. B.; Norcott, P. L.; Ciampi, S.; Coote, M. L., Effect of Chemical Structure on the Electrochemical Cleavage of Alkoxyamines. J. Phys. Chem. C 2019, 123, 5273-5281.
11. Fuchigami, T.; Inagi, S.; Atobe, M., Appendix B: Tables of Physical Data. In Fundamentals and Applications of Organic Electrochemistry, Fuchigami, T.; Inagi, S.; Atobe, M., Eds. John Wiley and Sons, Ltd.: 2015; pp 217-222.
12. Constantinides, C. P.; Koutentis, P. A., Chapter Seven - Stable N- and N/S-Rich Heterocyclic Radicals: Synthesis and Applications. In Advances in Heterocyclic Chemistry, Scriven, E. F. V.; Ramsden, C. A., Eds. Academic Press: 2016; Vol. 119, pp 173-207.
13. Lipunova, G. N.; Fedorchenko, T. G.; Chupakhin, O. N., Verdazyls: synthesis, properties, application. Russ. Chem. Rev. 2013, 82, 701-734.
14. Koivisto, B. D.; Hicks, R. G., The magnetochemistry of verdazyl radical-based materials. Coord. Chem. Rev. 2005, 249, 2612-2630.
15. Noble, B. B.; Norcott, P. L.; Hammill, C. L.; Ciampi, S.; Coote, M. L., Mechanism of Oxidative Alkoxyamine Cleavage: The Surprising Role of the Solvent and Supporting Electrolyte. J. Phys. Chem. C 2019, 123, 10300-10305.
16. Rogers, F. J. M.; Coote, M. L., Computational Evaluation of the Oxidative Cleavage of Triazine Derivatives for Electrosynthesis. J Phys. Chem. C 2019, 123, 10306-10310.
17. Rogers, F. J. M.; Coote, M. L., Computational Assessment of Verdazyl Derivatives for Electrochemical Generation of Carbon-Centered Radicals. J. Phys. Chem. C 2019, 123, 20174-20180.
18. Blinco, J. P.; Hodgson, J. L.; Morrow, B. J.; Walker, J. R.; Will, G. D.; Coote, M. L.; Bottle, S. E., Experimental and Theoretical Studies of the Redox Potentials of Cyclic Nitroxides. J. Org. Chem. 2008, 73, 6763-6771.
19. Zhang, K.; Noble, B. B.; Mater, A. C.; Monteiro, M. J.; Coote, M. L.; Jia, Z. F., Effect of heteroatom and functionality substitution on the oxidation potential of cyclic nitroxide radicals: role of electrostatics in electrochemistry. Phys. Chem. Chem. Phys. 2018, 20, 2606-2614.
20. Savva, A. C.; Mirallai, S. I.; Zissimou, G. A.; Berezin, A. A.; Demetriades, M.; Kourtellaris, A.; Constantinides, C. P.; Nicolaides, C.; Trypiniotis, T.; Koutentis, P. A., Preparation of Blatter Radicals via Aza-Wittig Chemistry: The Reaction of N-Aryliminophosphoranes with 1-(Het)aroyl-2-aryldiazenes. J. Org. Chem. 2017, 82, 7564-7575.
21. Berezin, A. A.; Zissimou, G.; Constantinides, C. P.; Beldjoudi, Y.; Rawson, J. M.; Koutentis, P. A., Route to Benzo- and Pyrido-Fused 1,2,4-Triazinyl Radicals via N′-(Het)aryl-N′-[2-nitro(het)aryl]hydrazides. J. Org. Chem. 2014, 79, 314-327.
22. Gilroy, J. B.; McKinnon, S. D. J.; Koivisto, B. D.; Hicks, R. G., Electrochemical Studies of Verdazyl Radicals. Org. Lett. 2007, 9, 4837-4840.
23. Frisch, M. J.; Trucks, G. W.; Schlegel, H. B.; Scuseria, G. E.; Robb, M. A.; Cheeseman, J. R.; Scalmani, G.; Barone, V.; Petersson, G. A.; Nakatsuji, H., et al. Gaussian 16 Rev. C.01, Wallingford, CT, 2016.
24. Werner, H.-J.; Knowles, P. J.; Manby, F. R.; Black, J. A.; Doll, K.; Heßelmann, A.; Kats, D.; Köhn, A.; Korona, T.; Kreplin, D. A., et al., The Molpro quantum chemistry package. J. Chem. Phys. 2020, 152, 144107.
25. Zhang, L.; Laborda, E.; Darwish, N.; Noble, B. B.; Tyrell, J. H.; Pluczyk, S.; Le Brun, A. P.; Wallace, G. G.; Gonzalez, J.; Coote, M. L., et al., Electrochemical and Electrostatic Cleavage of Alkoxyamines. J. Am. Chem. Soc. 2018, 140, 766-774.
26. Zhao, Y.; Truhlar, D. G., The M06 Suite of Density Functionals for Main Group Thermochemistry, Thermochemical Kinetics, Non-covalent Interactions, Excited States, and Transition

Elements: Two New Functionals and Systematic Testing of Four M06-class Functionals and 12 Other Functionals. Theor. Chem. Acc 2007, 120, 215-241.
27. Izgorodina, E. I.; Brittain, D. R. B.; Hodgson, J. L.; Krenske, E. H.; Lin, C. Y.; Namazian, M.; Coote, M. L., Should Contempory Density Functional Theory Methods be Used to Study the Thermodynamics of Radical Reactions? J. Phys. Chem. A 2007, 111, 10754–10768.
28. Ho, J.; Klamt, A.; Coote, L. M., Comment on the Correct Use of Continuum Solvent Models. J. Phys. Chem. A 2010, 114, 13442-13444.
29. Marenich, A. V.; Cramer, C. J.; Truhlar, D. G., Universal Solvation Model Based on Solute Electron Density and on a Continuum Model of the Solvent Defined by the Bulk Dielectric Constant and Atomic Surface Tensions. J. Phys. Chem. B 2009, 113, 6378-6396.
30. Marenich, A. V.; Ho, J.; Coote, M. L.; Cramer, C. J.; Truhlar, D. G., Computational Electrochemistry: Prediction of Liquid-Phase Reduction Potentials. Phys. Chem. Chem. Phys. 2014, 16, 15068-15106.
31. Haddon, R. C., Comment on the Relationship of the Pyramidalization Angle at a Conjugated Carbon Atom to the σ Bond Angles. J. Phys. Chem. A 2001, 105, 4164-4165.
32. Hodgson, J. L.; Namazian, M.; Bottle, S. E.; Coote, M. L., One-Electron Oxidation and Reduction Potentials of Nitroxide Antioxidants: A Theoretical Study. J. Phys. Chem. A 2007, 111, 13595-13605.
33. Gryn'ova, G.; Barakat, J. M.; Blinco, J. P.; Bottle, S. E.; Coote, M. L., Computational Design of Cyclic Nitroxides as Efficient Redox Mediators for Dye-Sensitized Solar Cells. Chem. Eur. J. 2012, 18, 7582-7593.
34. Kentaro, N.; Kenichi, O.; Hiroyuki, N., Organic Radical Battery Approaching Practical Use. Chem. Lett. 2011, 40, 222-227.
35. Suga, T.; Pu, Y.-J.; Kasatori, S.; Nishide, H., Cathode- and Anode-Active Poly(nitroxylstyrene)s for Rechargeable Batteries: p- and n-Type Redox Switching via Substituent Effects. Macromolecules 2007, 40, 3167-3173.
36. Janoschka, T.; Martin, N.; Hager, M. D.; Schubert, U. S., An Aqueous Redox-Flow Battery with High Capacity and Power: The TEMPTMA/MV System. Angew. Chem. Int. Ed. 2016, 55, 14427-14430.
37. Hansen, K.-A.; Nerkar, J.; Thomas, K.; Bottle, S. E.; O'Mullane, A. P.; Talbot, P. C.; Blinco, J. P., New Spin on Organic Radical Batteries–An Isoindoline Nitroxide-Based High-Voltage Cathode Material. ACS Appl. Mat. Int. 2018, 10, 7982-7988.
38. Charlton, G. D.; Barbon, S. M.; Gilroy, J. B.; Dyker, C. A., A bipolar verdazyl radical for a symmetric all-organic redox flow-type battery. J. Energ. Chem. 2019, 34, 52-56.
39. Muench, S.; Wild, A.; Friebe, C.; Häupler, B.; Janoschka, T.; Schubert, U. S., Polymer-Based Organic Batteries. Chem. Rev. 2016, 116, 9438-9484.
40. Friebe, C.; Lex-Balducci, A.; Schubert, U. S., Sustainable Energy Storage: Recent Trends and Developments toward Fully Organic Batteries. ChemSusChem 2019, 12, 4093-4115.
41. Hansen, K.-A.; Chambers, L. C.; Eing, M.; Barner-Kowollik, C.; Fairfull-Smith, K. E.; Blinco, J. P., A Methoxyamine-Protecting Group for Organic Radical Battery Materials—An Alternative Approach. ChemSusChem 2020, 13, 2386-2393.

Table of Contents Graphic